Available online at www.sciencedirect.com
ScienceDirect
Bioorganic & Medicinal Chemistry Letters 16 (2006) 6316–6320
Bioorganic & Medicinal Chemistry Letters

Discovery and design of benzimidazolone based inhibitors of p38 MAP kinase

Abdelhakim Hammach, Antonio Barbosa, Faith Corbo Gaenzler, Tazmeen Fadra, Daniel Goldberg, Ming-Hong Hao, Rachel R. Kroe, Pingrong Liu, Kevin C. Qian, Mark Ralph, Christopher Sarko, Fariba Soleymanzadeh and Neil Moss*

Departments of Medicinal Chemistry and Biologics and Biomolecular Sciences, Boehringer Ingelheim Pharmaceuticals, Inc., 900 Ridgebury Road, Ridgefield, CT 06877, USA

Received 24 July 2006; revised 31 August 2006; accepted 6 September 2006
Available online 28 September 2006

Abstract—A new class of benzimidazolone p38 MAP kinase inhibitors was discovered through high-throughput screening. X-ray crystallographic data of the lead molecule with p38 were used to design analogues with improved binding affinity and potency in a cell assay of LPS-induced TNFα production. Herein, we report the SAR of this new class of p38 inhibitors.

Tumor necrosis factor alpha (TNFα) and interleukin 1 (IL-1β) are pro-inflammatory cytokines implicated in many inflammatory diseases such as rheumatoid arthritis (RA), inflammatory bowel disease, and psoriasis. To date, several anti-TNFα biologics including Enbrel®, Remicade®, and Humira® have been approved by the FDA for use as anti-inflammatory therapies.[1] p38α is a mitogen activated protein (MAP) kinase that plays an essential role in the signal transduction pathways leading to the synthesis of TNFα and IL-1β.[2] Efforts from many pharmaceutical companies have led to the development of several p38 inhibitor clinical candidates, including our own BIRB 796 (**1**).[3]

As part of our ongoing efforts toward discovering alternative classes of p38α inhibitors that could be developed as backups to BIRB 796 (**1**), we conducted a high-throughput screening campaign against p38α and identified the benzimidazolone **2** as potentially interesting starting point (Fig. 1). Compound **2** displayed an IC_{50} in our high-throughput kinase assay of 130 nM and a thermal denaturation temperature (T_m)[4] with p38α of 50 °C. However, compound **2** did not inhibit TNFα production from LPS-stimulated THP-1 cells (Table 1).

We were fortunate to obtain X-ray crystallographic data of compound **2** bound to p38α (Figs. 2 and 3). Unlike the diaryl urea based inhibitor **1**, which binds to p38α in its Phe-out conformation,[3] compound **2** binds to p38α in its Phe-in conformation like many conventional p38α inhibitors.[2d] The NH and carbonyl of the benzimidazolone engage in H-bonding interactions with the carbonyl of His 107 and the NH of Met 109, respectively. These interactions are analogous to the H-bonding interactions typically seen between the adenine of ATP and a kinase. The unsubstituted phenyl group of the benzophenone portion of **2** occupies the so-called kinase specificity pocket (KSP) of p38α. The combination of the molecular potency of **2** together with the structural information from the X-ray structure encouraged us to initiate an SAR investigation of this class of p38 inhibitors.

The benzimidazolones **16**–**26** shown in Table 1 were synthesized from one of the 5-substituted-2-halo-nitrophenyl derivatives **10**, **11**, or **12** (representative examples shown in Scheme 1). Compounds **11** and **12** could be obtained in good yields via a copper mediated coupling of phenyl boronic acid **7** with 3-nitro-4-fluoroaniline **8** or with 3-nitro-4-chlorophenol **9**, respectively.[5] Thus as shown, reaction of **10**–**12** with cyclohexylmethylamine provided the 4-amino-3-nitro derivatives **13**–**15**. Subsequent reduction of the nitro group and condensation of the resultant diamine with carbonyldiimidazole

Keywords: p38 MAP kinase; Inhibitor; Benzimidazolone.
* Corresponding author. Tel.: +1 203 798 5101; fax: +1 203 791 6072; e-mail: nmoss@rdg.boehringer-ingelheim.com

0960-894X/$ - see front matter © 2006 Elsevier Ltd. All rights reserved.
doi:10.1016/j.bmcl.2006.09.014

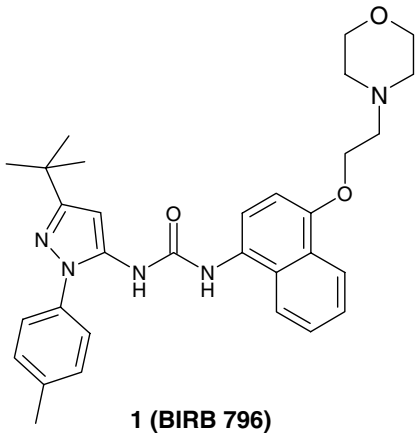

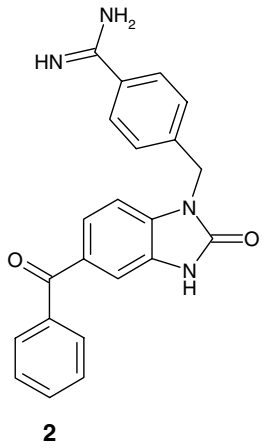

Figure 1. Structures of BIRB 796 (**1**) and the lead molecule **2**.

Table 1. Effect of the linker (X) and N1-substituents (R) on the binding affinity to p38α as measured by thermal denaturation temperature (T_m) and on the inhibition of TNFα from LPS stimulated THP-1 cells

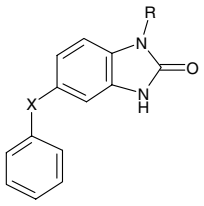

Entry	X	R	T_m[a] (°C)	Inhibition of TNFα from THP-1 cells EC_{50}[b] (nM)
2	–CO–	4-Guanylbenzyl–	50.3 ± 0.3	>10,000
3	–CO–	Ph-CH_2–	52.9 ± 0.4	1000
4	–CO–	Cyclohexyl-CH_2–	51.8	880
5	–CO–	CH_3–	49.1	>5000
6	–CO–	H–	48.0	>5000
16	–NH–	Cyclohexyl-CH_2–	54.0 ± 0.3	270
17	–O–	Cyclohexyl-CH_2–	53.2 ± 0.4	250
21	–NH–	*t*-Bu–	55.3	74
22	–NH–	$NH_2CH_2(CH_3)_2C$–	48.6 ± 0.1	3400
23	–NH–	Cyclopentyl–	55.3	150
24	–NH–	3-Pyrrolidinyl–	49.6 ± 0.1	1100
25	–NH–	2,6-di-F-Benzyl–	55.2	220
26	–NH–	Ph-CH_2–	54.2 ± 0.2	320

[a] Values with errors are from two experiments (range/2).
[b] Values are from one or two experiments (reproducibility in this assay observed with many compounds typically within ±50%).

yielded the benzimidazolones **4**, **16**, and **17**. The synthesis of compounds **22** and **24** required an additional Boc deprotection step to liberate the free amine.

Scheme 2 depicts the general approach used to functionalize the 6-position of the benzimidazolone core (synthesis of compound **36** used as an example). Copper mediated coupling of 2,4-difluoro-5-nitroaniline **18** with phenylboronic acid **7** afforded the difluoroaniline derivative **19**. Sequential and selective nucleophilic aromatic

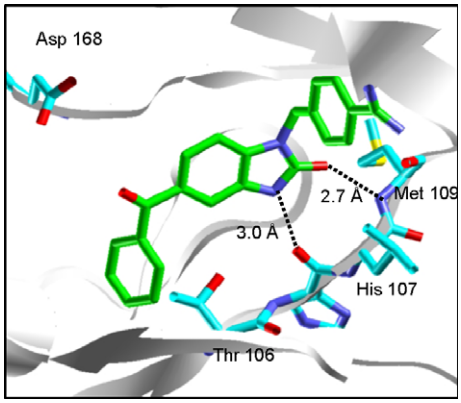

Figure 2. X-ray structure of **2** (green cylinder) complexed with p38α (Thr 106 to Met 109 as cyan cylinders) highlighting H-bond interactions between **2** and His 107 C=O and Met 109 NH.

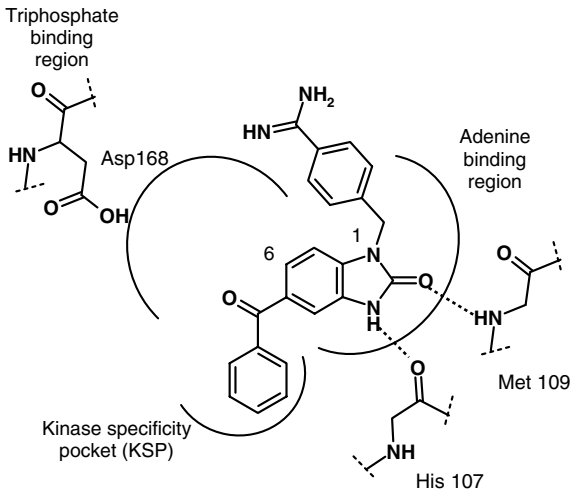

Figure 3. Representation of binding interactions observed from the complex of compound **2** with p38α.

substitutions of the two fluorine atoms were achieved by displacement of the 4-fluoro with cyclohexylmethylamine at room temperature, followed by displacement of the 2-fluoro with *N*-methylpiperazine at 100 °C, to

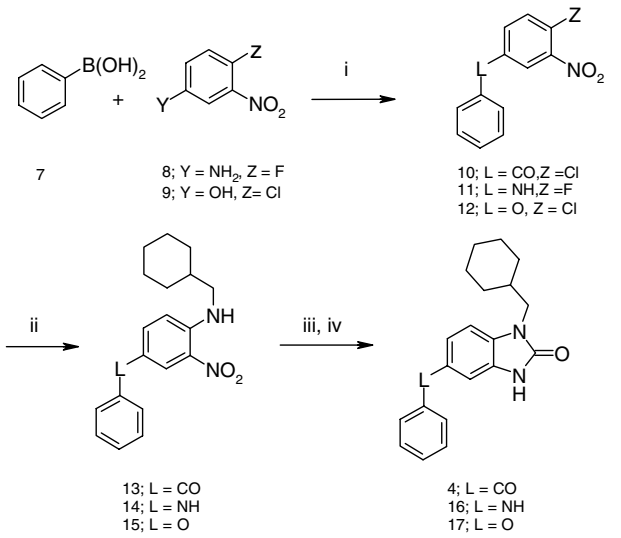

Scheme 1. Reagents and conditions: (i) for **11** and **12**, $Cu(OAc)_2$, NEt_3, CH_2Cl_2, rt, 48 h, 61 and 54%, respectively; (ii) Hunig's Base, DMF, cyclohexylmethylamine, 100 °C, 24 h, 59–73%; (iii) 10% Pd/C, H_2, EtOAc, rt, 16 h, 63–82%; (iv) 1,1′-carbonyldiimidazole, THF, 12 h, 65–78%.

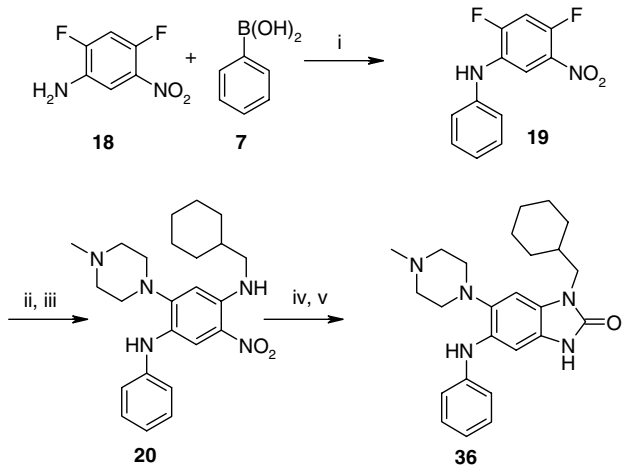

Scheme 2. Reagents and conditions: (i) $Cu(OAc)_2$, NEt_3, CH_2Cl_2, rt, 48 h, 91%; (ii) cyclohexylmethylamine, DMF, rt, 14 h, 90%; (iii) *N*-methylpiperazine, Hunig's Base, DMF, 100 °C, 24 h, 64%; (iv) 10% Pd/C, H_2, EtOAc, rt, 16 h, 75%; (v) 1,1′-carbonyldiimidazole, THF, 16 h, 65%.

provide the tetrasubstituted nitrophenyl derivative **20**. Reduction of the nitro group, followed by condensation with carbonyldiimidazole, provided the 5,6-diaminosubstituted benzimidazolone **36**. Compounds **35**–**38** were made in a similar manner.

X-ray crystallographic data of compound **2** bound to p38α showed that the benzyl guanidine substituent lay in a hydrophobic cleft leading up to the solvent front. However, the guanidine group itself was not involved in any particular interactions with the protein. Removal of this group resulted in an increase of 2.5 °C in the thermal denaturation assay (compound **3**, Table 1). Moreover, compound **3** proved efficacious in inhibiting TNFα production from LPS-stimulated THP-1 cells. While the saturated analogue **4** proved equipotent to compound **3**, truncation to the methyl or hydrogen analogues **5** and **6** resulted in a substantial decrease of potency and a complete loss of binding, respectively (compound **6** has a T_m equal to apo p38α[4]).

X-ray co-crystallographic data of **2** also showed that the oxygen atom of the benzophenone did not partake in any binding interactions with the protein. However, this carbonyl group does help link two key pharmacophores, the hydrogen bond donor/acceptor motif of the benzimidazolone, and the phenyl group which binds in the KSP. A comparison of the calculated relative energies of the bound conformation and the ground state conformation around the carbonyl region suggested the bound state conformation to be disfavored by about 1.5 kcal. We hypothesized that inhibitors with smaller linkers such as O or NH linker would decrease this energy difference and thus be more potent. Indeed, replacement of this carbonyl in **4** by an amino or an ether linker (compounds **16** and **17**) resulted in an increase of both molecular and cellular potency.

Further explorations off N1, now using compound **16** as a frame of reference, indicated a tolerance to various lipophilic groups (**21**, **23**, **25**, and **26**). However, modification of the N1 group with an amine function resulted in a substantial decrease in potency (cf. **21** and **22**; **23** and **24**), highlighting the incompatibility of such polar substituents in the hydrophobic cleft leading up to the solvent front.

Small substitutions on the phenyl ring of **16** (group that interacts with the KSP) were found to modestly improve molecular and cellular potency (Table 2). The 2,4-difluoro analogue **30** offered the best overall improvement increasing T_m by 2.8 °C and decreasing the EC_{50} in the TNFα cell assay by around 3- to 4-fold. In contrast, the 3-position appeared less tolerant to substitution (**31**–**33**).

With the aim of improving both the binding and the physicochemical properties of this class of p38α inhibitors, we investigated whether we could modify our compounds to take advantage of a potential interaction with Asp 168, located in the phosphate binding domain. The introduction of appropriately positioned basic substituents to gain interactions within the phosphate binding region has been reported to improve inhibitor potency for certain kinases.[6] Based on the observed binding conformation, we felt the 6-position of the benzimidazolone core offered the best directionality to position substitutions within binding distance to Asp 168 (Fig. 3). Unfortunately, introduction of either a piperazinyl (**35** and **37**) or the more flexible *N*-methyl-*N*′,*N*′-dimethylaminoethyl (**38**) led to a slight decrease in T_m (Table 2). Nevertheless, incorporation of a basic amine did significantly improve inhibitor aqueous solubility (5.7 μM for **36** vs 0.2 μM for **16** at pH 7.4).

Interestingly, X-ray crystallographic data of compound **38** with p38α show the dimethylamino group situated

Table 2. Effect of the substituents $(X)_n$ and R on the binding affinity to p38α as measured by thermal denaturation temperature (T_m) and on the inhibition of TNFα from LPS stimulated THP-1 cells

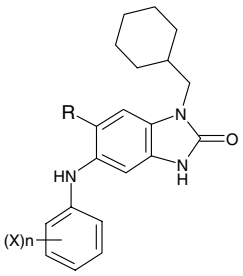

Entry	$(X)_n$	R	T_m[a] (°C)	Inhibition of TNFα from THP-1 cells EC_{50}[b] (nM)
16	H	H	54.0 ± 0.3	180
27	2-F	H	55.1 ± 0.1	66
28	3-F	H	52.1 ± 0.3	190
29	4-F	H	54.6 ± 0.2	74
30	2,4-di-F	H	56.8 ± 0.7	46
31	3,4-di-F	H	51.5 ± 0.3	420
32	3-CF_3	H	49.6 ± 0.1	2300
33	3,5-di-Cl	H	48.5 ± 1.2	>10,000
34	2-CH_3	H	55	64
35	H	Piperazinyl	52.8 ± 0.2	150
36	H	4-CH_3-piperazinyl	53.4 ± 0.2	150
37	2-CH_3	4-CH_3-piperazinyl	53.2	180
38	2-CH_3	*N*-Methyl-*N*′,*N*′-di-CH_3-aminoethyl	52.8	150

[a] Values with errors are from two experiments (range/2).
[b] Values are from one or two experiments (reproducibility in this assay observed with many compounds typically within ±50%).

within hydrogen-bonding distance from Asp 168 (Fig. 4). A comparison of the X-ray co-crystal structures of compounds **38** and **30** provides a potential rationale for the lack of observed improvement in molecular potency for **38** (Fig. 4). The co-crystal structure of compound **30** reveals an edge to face interaction between the aromatic side chain of Tyr 379 and the aromatic core of the benzimidazolone. In the co-crystal structure of compound **38**, neither Tyr 379 nor the entire glycine-rich loop to which this residue is attached is observed.

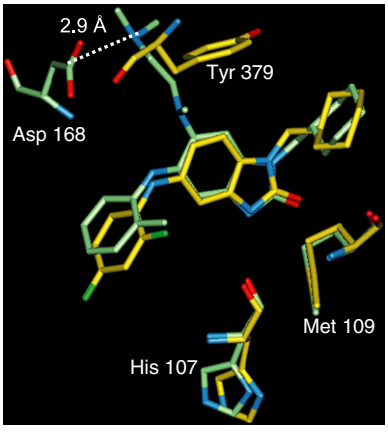

Figure 4. Overlay of p38α co-complexes of compounds **38** (green cylinder with residues Asp 168, His 107, and Met 109) and **30** (yellow cylinder with residues Asp 168, His 107, Met 109, and Tyr 379). The salt bridge (2.9 Å) between Asp 168 and the dimethylamino group of **38** highlighted.

Conceivably, in order to accommodate the *N*-methyl-*N*′,*N*′-dimethylaminoethyl group of compound **38**, Tyr 379 and the glycine-rich loop must be displaced, thereby losing the beneficial edge to face interaction between Tyr 379 and the aromatic core of the benzimidazolone.

Compound **30** possesses a very good overall kinase selectivity profile showing negligible inhibition of the following kinases when tested at 10 μM: Btk, Eck, EGFR, FGFR3, Hek, HGFR, IGF1R, IR, Itk, JAK3, Lyn, Syk, Tie-2, TXK, VEGFR1, MKK1, ERK2, JNK1, p38γ, p38δ, MAPKAP-K1α, MAPKAP-K2, MSK1, PRAK, PKA, PKCα, PDK1, PKBδPH, SGK, S6K1, GSK3β, ROCK-II, AMPK, CHK1, CK2, PHOS. KINASE, LCK, CSK, CDK2/cyclin A, CK1, DYRK 1A, PP2A, NEK6. Compound **30** shows similar inhibition of p38β at 10 μM as seen for p38α (dose down not done). It is noteworthy that compound **30** shows selectivity even against Jnk2α2, a kinase frequently inhibited by other classes of p38α inhibitors. Compound **30** inhibits Jnk2α2 with an IC_{50} of 5.5 μM, whereas BIRB 796 (**1**) inhibits this enzyme with an IC_{50} of 0.006 μM.

In conclusion, X-ray crystallographic data of **2** with p38α were exploited to improve the binding of the benzimidazolone class of p38α inhibitors culminating in compound **30**. Most notable were the improvements in binding and cellular potency resulting from replacing the carbonyl of the benzophenone with an amino-linker and optimizing the lipophilic interactions within the kinase specificity pocket.

References and notes

1. (a) Klinkhoff, A. *Drugs* **2004**, *64*, 1267; (b) Barry, J.; Kirby, B. *Expert Opin. Biol. Ther.* **2004**, *4*, 975.
2. (a) Saklatvala, J. *Curr. Opin. Pharm.* **2004**, *4*, 372; (b) Kumar, S.; Boehm, J.; Lee, J. C. *Nat. Rev. Drug Discov.* **2003**, *2*, 717; (c) Ono, K.; Han, J. *Cell. Signalling* **2000**, *12*, 1; (d) Jakckson, P. F.; Bullington, J. L. *Curr. Top. Med. Chem.* **2002**, *2*, 1009; (e) Cirillo, P.; Pargellis, C.; Regan, J. *Curr. Top. Med. Chem.* **2002**, *2*, 1021.
3. (a) Regan, J.; Breitfelder, S.; Cirillo, P.; Gilmore, T.; Graham, A. G.; Hickey, E. R.; Klaus, B.; Madwed, J.; Moriak, M.; Moss, N.; Pargellis, C. A.; Pav, S.; Proto, A.; Swinamer, A.; Tong, L.; Torcellini, C. *J. Med. Chem.* **2002**, *45*, 2994; (b) Regan, J.; Capolino, A.; Cirillo, P. F.; Gilmore, T.; Graham, A. G.; Hickey, E.; Kroe, R. R.; Madwed, J.; Moriak, M.; Nelson, R.; Pargellis, C. A.; Swinamer, A.; Torcellini, C.; Tsang, M.; Moss, N. *J. Med. Chem.* **2003**, *46*, 4676.
4. Kroe, R. R.; Regan, J.; Proto, A.; Peet, G. W.; Roy, T.; Dickert, L.; Fuschetto, N.; Pargellis, C. A.; Ingraham, R. H. *J. Med. Chem.* **2003**, *46*, 4669, The formula used in this reference to convert thermal denaturation temperatures (T_m) to binding affinities (K_d) applies to a Phe-out class of p38 inhibitors and consequently cannot be accurately applied to the Phe-in class of inhibitors in this paper. Thus to allow the reader to approximate conversions of T_m values to kinase assay IC_{50}s, we provide the T_m values determined for a range of known Phe-in p38 inhibitors.

Compound	Reported Kinase assay IC_{50} (nM)	Determined T_m (°C)
Roche RO 3201195	700	50.7
SmithKline SB203580	40	54.9
Vertex VX-745	20	55.9
Merck L 779,450	0.1	59.5

The IC_{50}s for RO3201195, SB203580, VX-745, and L779,450 have been disclosed in the following references, respectively. Goldstein, D. M.; Gabriel, T. *Curr. Top. Med. Chem.* **2005**, *5*, 1017; (b) Lee, J. C.; Laydon, J. T.; McDonnell, P. C.; Gallageher, T. F.; Kumar, S.; Green, D.; Blumenthal, M. J.; Heys, J. R.; Landvatter, S. W.; Strickler, J. E.; McLaughlin, M. M.; Siemens, I. R.; Fisher, S. M.; Livi, G. P.; White, J. R.; Adams, J. L.; Young, P. R. *Nature* **1994**, *372*, 739; (c) Salutoro, F. G. In *27th National Medicinal Chemistry Symposium*, Kansa City, MO, June 13–17, 2000; (d) Liverton, N. J.; Butcher, J. W.; Claiborne, C. F.; Claremon, D. A.; Libby, B. E.; Nguyen, K. T.; Pitzenberger, S. M.; Selnick, H. G.; Smith, G. R.; Tebben, A.; Vacca, J. P.; Varga, S. L.; Agarwal, L.; Dancheck, K.; Forsyth, A. J.; Fletcher, D. S.; Frantz, B.; Hanlon, W. A.; Harper, C. F.; Hofsess, S. J.; Kostura, M.; Lin, J.; Luell, S.; O'Neill, E. A.; Orevillo, C. J.; Pang, M.; Parsons, J.; Rolando, A.; Sahly, Y.; Visco, D. M.; O'Keefe, S. J. *J. Med. Chem.* **1999**, *42*, 2180.
5. (a) Chan, D. M. T.; Monaco, K. L.; Wang, R. P.; Winters, M. P. *Tetrahedron Lett.* **1998**, *39*, 2933; (b) Lam, P. Y. S.; Clark, C. G.; Saubern, S.; Adams, J.; Winters, M. P.; Chan, D. M. T.; Combs, A. *Tetrahedron Lett.* **1998**, *39*, 2941; (c) Evans, D. A.; Katz, J. L.; West, T. R. *Tetrahedron Lett.* **1998**, *39*, 2937; (d) Lam, P. Y. S.; Clark, C. G.; Saubern, S.; Adams, J.; Averill, K.; Chan, D. M. T.; Combs, A. P. *Synlett* **2000**, 674.
6. (a) Revesz, L.; Blum, E.; Di Padova, F. E.; Buhl, T.; Feifel, R.; Gram, H.; Hiestand, P.; Manning, U.; Rucklin, G. *Bioorg. Med. Chem. Lett.* **2004**, *14*, 3601; (b) Revesz, L.; Di Padova, F. E.; Buhl, T.; Feifel, R.; Gram, H.; Hiestand, P.; Manning, U.; Wolf, R.; Zimmerlin, A. G. *Bioorg. Med. Chem. Lett.* **2002**, *12*, 2109; (c) Moffat, D.; Davis, P.; Hutchings, M.; Davis, J.; Berg, D.; Batchelor, M.; Johnson, J.; O'Connell, J.; Martin, R.; Carabbe, T.; Delgado, J.; Perry, M. *Bioorg. Med. Chem. Lett.* **1999**, *9*, 3351.